Mollow-like Triplets in Ultrafast Resonant Absorption

Axel Stenquist,[1] Felipe Zapata,[2,*] Edvin Olofsson,[1] Yijie Liao,[3] Elna Svegborn,[1] Jakob Nicolai Bruhnke,[1] Claudio Verdozzi,[1] and Jan Marcus Dahlström[1,†]

[1]Department of Physics, Lund University, 22100 Lund, Sweden
[2]Departamento de Química, Universidad Autónoma de Madrid, 28049 Madrid, Spain
[3]School of Physics and Wuhan National Laboratory for Optoelectronics, Huazhong University of Science and Technology, Wuhan, 430074, China

(Received 28 March 2024; revised 29 May 2024; accepted 9 July 2024; published 9 August 2024)

We show that resonant absorption of smooth laser fields can yield Mollow-like triplet patterns. General conditions for such triplets are derived and illustrated with a super-Gaussian pulse sequence. Gaussian pulses cannot exhibit triplets, super-Gaussian pulses can form triplets depending on the pulse area, and flattop pulses can produce absorption triplets after one Rabi cycle. Our results are compared side by side with resonance fluorescence to emphasize similarities and differences between these unlike observables. In the high-intensity limit, we show that the central absorption peak is asymmetric, which we attribute to nonlinear photoionization, beyond two-level atomic physics.

DOI: 10.1103/PhysRevLett.133.063202

Mollow triplet formation is a well-known phenomenon in resonance fluorescence from atoms [1], with a characteristic three-peaked spectrum. The structure can be understood from the dressed-state picture with quantum electrodynamics (QED) for continuous wave lasers [2,3], where adjacent peaks are separated by the Rabi frequency. While Mollow triplets in resonance fluorescence have been observed in many quantum systems, such as highly charged ions [4], cold atoms [5], and quantum dots [6,7], and in optically confined atoms [8], the phenomenon has been predicted to be strongly modified for smooth laser pulses of finite duration due to interference of photons from different times [4,9–14]. Experimental evidence for such dynamically dressed states by resonance fluorescence was recently found in quantum dots [15,16].

During the last decade, transient absorption spectroscopy has been used to measure coherent electronic dynamics in atoms and molecules with unprecedented resolution down to the attosecond timescale [17–29]. However, Mollow-like absorption triplets have so far not been reported. This may be due to inadequate laser conditions that could prevent such effects from manifesting in absorption driven by strong laser fields, or due to some unknown physical restrictions. The rapid development of seeded extreme ultraviolet free electron lasers (XUV-FEL), such as FERMI [30], opens up for such studies, as evidenced by the recent observation of dressed-states between helium atoms and light at XUV wavelengths [31,32]. Whether Mollow-like triplets in absorption spectra can be generated from seeded XUV-FEL pulses is thus a timely question that requires theoretical attention.

In this Letter, we employ strong-field transient absorption theory [26,27] for resonant XUV-FEL pulses in hydrogen atoms to elucidate the conditions for Mollow-like absorption triplets, resolved over the time, intensity, and the shape of the laser pulse. Our results for absorption are compared with QED calculations for resonance fluorescence [9,10], showing both remarkable similarities and stark differences between these two unlike observables (see insert in Fig. 1). In contrast to fluorescence, we show that the triplet structure in absorption is only formed when two seemingly opposing conditions can be simultaneously fulfilled. To study the dynamic buildup of Mollow-like absorption features, we consider the prototypical $1s-2p$ transition in hydrogen, which has a resonant energy of $\omega = 10.2$ eV, and a transition dipole element $z_0 = 0.745$. Atomic units are used throughout this text, $e = \hbar = m = 4\pi\epsilon_0 = 1$, unless otherwise stated.

Theory—Absorption of light is computed semiclassically using the fundamental energy conservation condition between the atom and the driving laser field, $\mathcal{E} = \mathcal{E}_{\mathrm{A}}(t) + \mathcal{E}_{\mathrm{L}}(t)$, following Wu *et al.* [26]. The time-dependent energy gain of the atom, $\Delta\mathcal{E}_{\mathrm{A}}(t) = -\Delta\mathcal{E}_{\mathrm{L}}(t)$, can be formally associated with Yang's energy operator [38], to write the theory in a gauge-invariant time-dependent form [27]. The exact electron dynamics of a hydrogen atom is computed, within the dipole

*Contact author: felipe.zapata@uam.es
†Contact author: marcus.dahlstrom@matfys.lth.se

approximation, by solving the time-dependent Schrödinger equation

$$i\frac{d}{dt}|\Psi(t)\rangle = [H_0 + V(t)]|\Psi(t)\rangle, \tag{1}$$

where $H_0 = \mathbf{p}^2/2 - 1/r$ is the hydrogen Hamiltonian and $V(t) = zE(t)$ is the semiclassical interaction term. The electric field is linearly polarized along the z direction and is defined by $E(t) = -\dot{A}$, with $A(t) = A_0\Lambda_n(t)\sin(\omega_0 t)$, where A_0 and ω_0 are the amplitude and central frequency, respectively. The pulse envelope is defined using the super-Gaussian sequence [10] as

$$\Lambda_n(t) = \exp\left[-\frac{\ln(2)}{2}\left(\frac{2t}{\tau}\right)^{2n}\right], \tag{2}$$

where τ is the pulse duration and $n = 1, 2, \ldots$ the index of the sequence. Here, $n = 1$ corresponds to the commonly used Gaussian pulse, while the limit $n \to \infty$ corresponds to gradual transformation to a flattop pulse.

The time-dependent velocity expectation value is computed as $\mathbf{v}(t) = \langle\Psi(t)|\mathbf{v}|\Psi(t)\rangle$. In the frequency domain, the energy gain is resolved as [27]

$$\Delta\tilde{\mathcal{E}}_A(\omega) = -2\mathrm{Re}[\tilde{v}_z(\omega)\tilde{E}^*(\omega)], \tag{3}$$

where ω is the angular frequency, and $\tilde{v}_z(\omega)$ and $\tilde{E}(\omega)$ are the Fourier transforms of the velocity expectation value (along z) and the electric field, respectively.

In order to interpret the atomic dynamics we make use of the well-known two-level physics [39]. The Rabi flopping of a two-level atom follows the pulse area, $\theta = \int \Omega(t)dt$, where $\Omega(t) \approx \omega_0 A_0 \Lambda_n(t) z_0$ is the time-dependent Rabi frequency. We have verified that the two-level model is in excellent agreement with our exact results at 10^{12} W/cm^2, and below. Therefore, we present our results in terms of completed Rabi cycles: $\theta/2\pi$. Further details are given in the Supplemental Material [33] (see also Refs. [34–37] therein).

Results—The pulse area of 3π is of particular interest. Physically, this corresponds to the atom being excited, de-excited, and re-excited by the laser field with net absorption of one photon (ω_0) at the end of the laser pulse. The corresponding results for absorption and resonant fluorescence with a flattop ($n \to \infty$), super-Gaussian ($n = 2$), and Gaussian ($n = 1$) envelope are presented in the first row of Fig. 1. In the following we will present results for each envelope in turn: (a)–(c).

Flattop: Three strong absorption peaks (black) are observed in remarkable agreement with the corresponding resonance fluorescence result (red dashed); see Fig. 1(a). Resonance fluorescence is here a non-negative quantity,

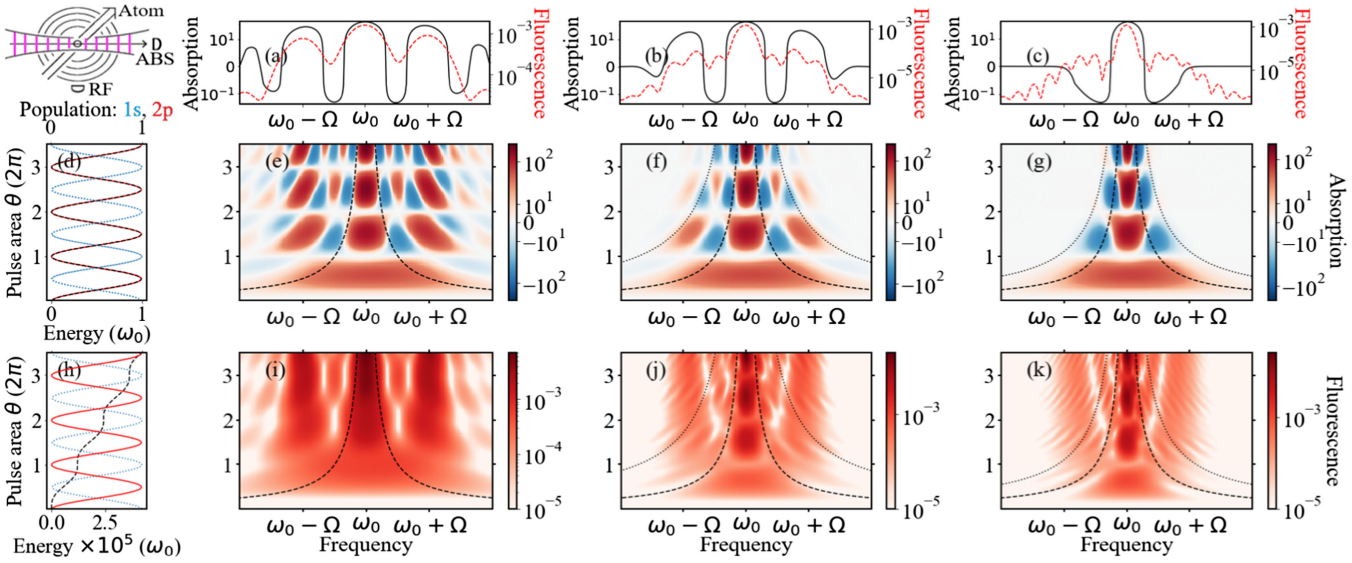

FIG. 1. Absorption (ABS) and resonant fluorescence (RF) spectra are presented for a fixed intensity of the laser, $I = 10^{12}$ W/cm^2, yielding the Rabi period $T_{\mathrm{Rabi}} = 38$ fs. In the top left, an illustration of ABS and RF measurements is presented. First row: line outs present the ABS (black) and RF (red dashed) for 3/2 Rabi cycles (3π pulse area) in (a), (b), and (c), for a flattop, super-Gaussian, and Gaussian envelope, respectively. Second row: ABS, resolved over pulse area, (d) showing the number of absorbed photons (black dashed) and the population of the excited (red) and ground state (blue dotted) for a flattop pulse. Panels (e), (f), and (g) show the frequency-resolved ABS for the flattop, super-Gaussian, and Gaussian pulse shapes, respectively, in symmetric logarithmic scale. ABS is computed with a filter function equal to the pulse envelope. Third row: RF, resolved over pulse area, calculated by a model based on QED [9,10], and scaled using the classically emitted radiation; see Supplemental Material [33]. The heat maps are superposed with dashed lines that describe the energy width of the central peak of the field, $2\pi/\tau$, and with dotted lines that describe a larger width of the pulse, $2\pi/\tau'_n$; see Fig. 2 and main text.

because it only concerns emission of light; see schematic in Fig. 1. In contrast, absorption can take positive and negative values due to interference between the incident laser pulse and the stimulated emission, in agreement with the pioneering work by Mollow for two-level atoms relaxed in monochromatic light subject to a perturbative auxiliary field [40]. In our time-resolved nonperturbative approach, shown in (d), the energy absorbed by the atom modulates periodically by exchange of one photon (black dashed), following closely the excited state population (red). In (e) we show the frequency-resolved absorption from a flattop pulse. Below one Rabi period, a single broad absorption peak is observed, which vanishes completely for a pulse area of exactly one Rabi period because the atom is driven back to the ground state. For pulse areas greater than 1, we first observe a Mollow-like absorption triplet at 1.5 Rabi cycles. At 2.5 Rabi cycles, a new structure is formed with an additional weaker absorption peak in between the sidebands and the main peak. At 3.5 Rabi cycles, there are two additional absorption peaks on either side of the main absorption peak.

Super-Gaussian: Three Mollow-like absorption peaks (black) are observed at 1.5 Rabi cycles in Fig. 1(b). However, this traditional-looking Mollow structure is a special case that only occurs for the 3π-area super-Gaussian pulse. This becomes clear when studying the frequency-resolved absorption, as a function of the pulse area, shown in Fig. 1(f). Above 2 Rabi cycles, the structure deviates completely from the Mollow triplet, because the prominent sidebands, positioned at $\omega_0 \pm \Omega_0$, are lacking or inferior to more narrow sidebands. Thus, at large pulse areas, the sidebands of super-Gaussian envelopes do not correspond to Mollow-like absorption structure.

Gaussian: At 1.5 Rabi cycle area the absorption spectrum shows only a single peak with two emission peaks (negative absorption) on either side as shown in Fig. 1(c). In (g) we show that the frequency-resolved absorption over the pulse area maintains this shape, with the expected narrowing of the central peak due to the time-bandwidth product. Revivals of absorption are found at 2.5 and 3.5 Rabi cycles. All side peaks from the super-Gaussian case (f) have vanished in the Gaussian case (g). This implies that the Gaussian pulse can not support the 3π-area Mollow triplet formation observed in the super-Gaussian case. Instead, the spectrum exhibits a central absorption peak and two emission peaks—a distinct feature that is different from Mollow triplet formation.

Fluorescence: In contrast to absorption, energy lost by resonance fluorescence is very small and increases approximately linearly with the pulse area (for fixed intensity), as shown in (h). We find that the energy lost through fluorescence is negligible (5 orders of magnitude smaller than the absorption), validating the fundamental assumption for energy conservation of the combined semiclassical atom and laser system, $\mathcal{E}$, [26,27]. Similarly, this also validates the

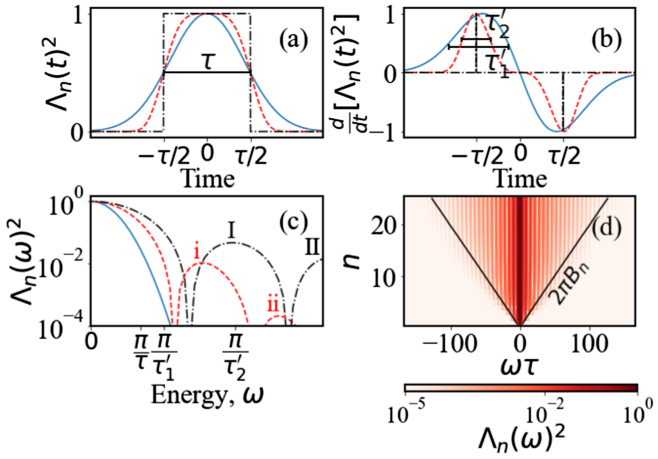

FIG. 2. Pulse structure characterized by pulse duration, τ, and *turn-on/off* duration, τ_n'. Three pulses in the super-Gaussian sequence, given by Eq. (2), are shown: Gaussian ($n = 1$) (blue), super-Gaussian ($n = 2$) (red dashed), and flattop ($n \to \infty$) (black dash-dotted). The squared envelope (a) and its derivative (b) are presented with the corresponding characteristic times, $\tau > \tau_n'$. (c) Squared Fourier transformed envelope with energy half width of the central component, π/τ, and a larger measure for the width, π/τ_n'. (d) Same as (c) resolved over super-Gaussian index n, where black lines are $\pm\pi\tau/\tau_n' = \pm 2\pi\mathcal{B}_n$.

omission of back action in QED from fluorescent photons [9,10], thus circumventing the need for more complete QED treatment, c.f. Ref. [11]. The Mollow triplet in fluorescence forms with the expected strong central peak and two sidebands, as shown in (i). We note that the weak final state dependency [13,15] is in strong contrast with our absorption results (e). In between the central peak and the sidebands, the Mollow structure develops additional peaks at 3 Rabi cycles (i), reminiscent of the additional absorption peaks observed at 2.5 Rabi cycles in (e). In the super-Gaussian (j) and Gaussian (k) cases the fluorescence shows a more complex structure with a central peak with broad wings on either side, which exhibits rich interference fringes [13,15,16]. In contrast to the fluorescence, associated to QED, the absorption is very different as it is not perturbative, but follows instantaneously the population of the excited state on the femtosecond timescale, as observed in (d).

Discussion—The considered pulse envelopes, $\Lambda_n(t)$, are illustrated in Figs. 2(a) and 2(b) with their pulse duration, τ, and *turn-on/off* duration, τ_n'. To understand the envelope dependence of the resonant absorption, presented in Figs. 1(e)–1(g), we must appreciate these two different timescales of the envelopes, τ and τ_n', which are associated with different widths in the frequency domain, $2\pi/\tau$ and $2\pi/\tau_n'$, as shown in Figs. 2(c) and 2(d). The central peak of the Gaussian is narrower in energy than the super-Gaussian and flattop cases, and its half spectral width is well estimated as π/τ (at which point its square has decreased by 2 orders of magnitude). The Gaussian also maintains its functional identity from time to energy, which explains

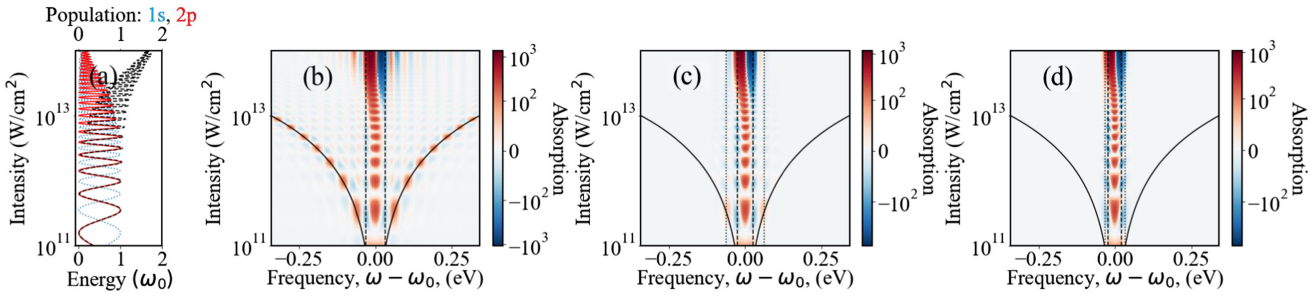

FIG. 3. Absorption spectra resolved over intensity, in the interval $I = 10^{11}$–10^{14} W/cm^2 for the pulse duration $\tau = 97$ fs. The number of absorbed photons (black dashed) and the population of the excited (red) and ground state (blue dotted), for interaction with a flattop pulse, is shown in (a). We observe two photon absorption for high intensity due to photoionization. Frequency-resolved absorption is shown in (b), (c), and (d) for a flattop, super-Gaussian ($n = 2$) and Gaussian pulse, respectively. Full black lines denote the energies $\pm\Omega$, i.e., the Mollow triplet separation, dashed vertical lines are the energy width of the field's central component π/τ, and dotted lines are the full Fourier width of the pulse π/τ_n'.

why it does not exhibit any modulations in the energy domain beyond the primary peak in contrast to the other envelopes shown. The shorter turn-on/off duration of a super-Gaussian pulse leads to frequency modulations, labeled by i and ii in Fig. 2(c). These additional peaks in the frequency domain are rather weak (its square decreases by 2 orders between adjacent maxima). For the flattop pulse, the turn-on/off effect is much more significant, and it leads to several additional Fourier peaks on the same order of magnitude, labeled by I and II. It is the presence of such modulations in the frequency domain that enables absorption features at large separations from the central frequency, by Eq. (3); see Fig. 2(d).

We find that a pulse can support the Mollow-like absorption peaks under two conditions: (i) the atom must undergo one Rabi cycle, $\theta > 2\pi$. In the frequency domain, this first condition implies that the bandwidth of the pulse is narrow enough to resolve the Rabi frequency. Combining the pulse area, $\theta = \Omega_0 \int \Lambda_n(t)dt$, where $\Omega_0 = 2\pi/T_{\mathrm{Rabi}}$, with the flattop pulse area, $\int \Lambda_\infty(t)dt = \tau$, yields the condition for the lower bound of the pulse duration $\tau > \mathcal{A}_n T_{\mathrm{Rabi}}$, where the dimensionless area constant is defined as $\mathcal{A}_n = \int \Lambda_\infty(t)dt / \int \Lambda_n(t)dt$. (ii) The pulse bandwidth must extend over the Rabi frequency, $\pi/\tau_n' > \Omega_0 \Leftrightarrow \tau < T_{\mathrm{Rabi}}\mathcal{B}_n$, where we introduce a dimensionless constant, $\mathcal{B}_n = \tau/2\tau_n' \approx 0.8n$; see Fig. 2(d). Thus, the Mollow-like structure can only develop under the general condition

$$\mathcal{A}_n < \tau/T_{\mathrm{Rabi}} < \mathcal{B}_n. \tag{4}$$

From this condition we find that Gaussian pulses cannot support Mollow-like absorption triplets, since $\mathcal{A}_1 = 1.50 > \mathcal{B}_1 = 0.735$. For the super-Gaussian ($n = 2$) case, however, the condition can be fulfilled, since $\mathcal{A}_2 = 1.18 < \mathcal{B}_2 = 1.45$, which allows for the first Mollow-like absorption triplet at $\theta/2\pi \approx 1.5$ in Fig. 1(f). For increasing super-Gaussian order, the condition is further relaxed. For the flattop case ($n \to \infty$), the turn-on time is infinitesimal, hence $\mathcal{A}_\infty = 1 < \mathcal{B}_n \to \infty$, which suggests that the modulations of the Fourier transform support Mollow-like absorption peaks at areas larger than one Rabi cycle, $\theta/2\pi > 1$, in agreement with our observations in Fig. 1(e). Here, multiple peaks are resolved on a color scale that maps the first 2 orders of magnitude, each corresponding to the Fourier peaks I, II, etc., from Fig. 2(c); see also (d).

The role of intensity: The resonant absorption for different pulse intensities is presented in Fig. 3. At low intensity, we see one photon absorption (black dashed line) in (a). As the intensity is increased, the stronger interaction with the laser leads to exchange energies beyond one photon, entering into the photoionization regime. Ionization yields decreased atomic two-level populations as seen in the excited (ground) state population marked with a red (blue dotted) line. The frequency-resolved absorption spectra are shown in (b), (c), and (d) for interaction with a flattop, super-Gaussian, and Gaussian pulse, respectively. We observe that the flattop case supports Mollow-like absorption triplets at all considered intensities. At very high intensity, however, the structure of the main peak changes into an asymmetric shape, with absorption below and emission above the resonant frequency, presenting a Fano-like profile. This asymmetric shape can be reproduced well by the damping of the amplitudes in an effective Hamiltonian two-level model; see Supplemental Material [33]. In the super-Gaussian case (c), only the first absorption triplet is formed (3π-area pulse), in agreement with Eq. (4). Finally, in the Gaussian case (d), a single absorption peak is observed with emission structures on either side. Similar to the flattop case (b), both the super-Gaussian (c) and Gaussian (d) cases exhibit a Fano-like asymmetric main absorption peak.

Conclusions—In this Letter, we have presented the conditions for Mollow-like triplets in resonant absorption of smooth laser fields. It was found that Gaussian pulses cannot exhibit the triplet phenomenon, while

super-Gaussian and flattop pulses can produce triplets in absorption. However, the triplet structure of super-Gaussian pulses depends on the pulse area, which is a phenomenon beyond the usual Mollow picture. A side-by-side comparison with resonance fluorescence was made to emphasize the stark differences in the unlike physical observables. Our work, which lies on the boundary between semiclassical physics and QED, motivates experiments to study absorption of intense seeded XUV-FEL pulses, opening the possibility of probing ultrafast dynamics in single- and multiphoton regimes in complex targets, such as molecules [41–43] and highly charged ions [44]. Finally, a natural extension of the present work is developing a fully quantum treatment of the absorption theory as an addition to the active fields of strong-field QED [45,46].

Acknowledgments—J. M. D. acknowledges support from the Olle Engkvist Foundation (194-0734) and the Knut and Alice Wallenberg Foundation (2019.0154). C. V. acknowledges support from the Swedish Research Council (Grant No. 2022-04486). F. Z. acknowledges support from the Ministerio de Universidades, el Plan de Recuperación, Transformación y Resilencia y la Universidad Autónoma de Madrid (CA1/RSUE/2021-00352) and the MSCA H2020 programme (101034324).

[1] B. R. Mollow, Power spectrum of light scattered by two-level systems, Phys. Rev. **188**, 1969 (1969).
[2] C. Cohen-Tannoudji and S. Reynaud, Modification of resonance Raman scattering in very intense laser fields, J. Phys. B **10**, 365 (1977).
[3] H. J. Kimble and L. Mandel, Theory of resonance fluorescence, Phys. Rev. A **13**, 2123 (1976).
[4] S. M. Cavaletto, C. Buth, Z. Harman, E. P. Kanter, S. H. Southworth, L. Young, and C. H. Keitel, Resonance fluorescence in ultrafast and intense x-ray free-electron-laser pulses, Phys. Rev. A **86**, 033402 (2012).
[5] L. Ortiz-Gutiérrez, R. C. Teixeira, A. Eloy, D. Ferreira Da Silva, R. Kaiser, R. Bachelard, and M. Fouché, Mollow triplet in cold atoms, New J. Phys. **21**, 093019 (2019).
[6] A. Ulhaq, S. Weiler, S. M. Ulrich, R. Roßbach, M. Jetter, and P. Michler, Cascaded single-photon emission from the Mollow triplet sidebands of a quantum dot, Nat. Photonics **6**, 238 (2012).
[7] A. Ulhaq, S. Weiler, C. Roy, S. M. Ulrich, M. Jetter, S. Hughes, and P. Michler, Detuning-dependent Mollow triplet of a coherently-driven single quantum dot, Opt. Express **21**, 4382 (2013).
[8] B. L. Ng, C. H. Chow, and C. Kurtsiefer, Observation of the Mollow triplet from an optically confined single atom, Phys. Rev. A **106**, 063719 (2022).
[9] K. Rzążewski and M. Florjanczyk, The resonance fluorescence of a two-level system driven by a smooth pulse, J. Phys. B **17**, L509 (1984).
[10] M. Florjanczyk, K. Rzążewski, and J. Zakrzewski, Resonance scattering of a short laser pulse on a two-level system: Time-dependent approach, Phys. Rev. A **31**, 1558 (1985).
[11] M. Lewenstein, J. Zakrzewski, and K. Rzążewski, Theory of fluorescence spectra induced by short laser pulses, J. Opt. Soc. Am. B **3**, 22 (1986).
[12] M. Lewenstein and L. You, Probing Bose-Einstein condensed atoms with short laser pulses, Phys. Rev. Lett. **71**, 1339 (1993).
[13] A. Moelbjerg, P. Kaer, M. Lorke, and J. Mørk, Resonance fluorescence from semiconductor quantum dots: Beyond the Mollow triplet, Phys. Rev. Lett. **108**, 017401 (2012).
[14] E. Viñas Boström, A. D'Andrea, M. Cini, and C. Verdozzi, Time-resolved multiphoton effects in the fluorescence spectra of two-level systems at rest and in motion, Phys. Rev. A **102**, 013719 (2020).
[15] K. Boos *et al.*, Signatures of dynamically dressed states, Phys. Rev. Lett. **132**, 053602 (2024).
[16] S. Liu, C. Gustin, H. Liu, X. Li, Y. Yu, H. Ni, Z. Niu, S. Hughes, X. Wang, and J. Liu, Dynamic resonance fluorescence in solid-state cavity quantum electrodynamics, Nat. Photonics **18**, 318 (2024).
[17] E. Goulielmakis *et al.*, Real-time observation of valence electron motion, Nature (London) **466**, 739 (2010).
[18] H. Wang, M. Chini, S. Chen, C.-H. Zhang, F. He, Y. Cheng, Y. Wu, U. Thumm, and Z. Chang, Attosecond time-resolved autoionization of argon, Phys. Rev. Lett. **105**, 143002 (2010).
[19] A. Wirth *et al.*, Synthesized light transients, Science **334**, 195 (2011).
[20] C. Ott, A. Kaldun, P. Raith, K. Meyer, M. Laux, J. Evers, C. H. Keitel, C. H. Greene, and T. Pfeifer, Lorentz meets fano in spectral line shapes: A universal phase and its laser control, Science **340**, 716 (2013).
[21] C. Ott *et al.*, Reconstruction and control of a time-dependent two-electron wave packet, Nature (London) **516**, 374 (2014).
[22] A. R. Beck, D. M. Neumark, and S. R. Leone, Probing ultrafast dynamics with attosecond transient absorption, Chem. Phys. Lett. **624**, 119 (2015).
[23] P. Birk, V. Stooß, M. Hartmann, G. D. Borisova, A. Blättermann, T. Heldt, K. Bartschat, C. Ott, and T. Pfeifer, Attosecond transient absorption of a continuum threshold, J. Phys. B **53**, 124002 (2020).
[24] H. J. B. Marroux, A. P. Fidler, A. Ghosh, Y. Kobayashi, K. Gokhberg, A. I. Kuleff, S. R. Leone, and D. M. Neumark, Attosecond spectroscopy reveals alignment dependent core-hole dynamics in the ICl molecule, Nat. Commun. **11**, 5810 (2020).
[25] P. Rupprecht *et al.*, Laser control of electronic exchange interaction within a molecule, Phys. Rev. Lett. **128**, 153001 (2022).
[26] M. Wu, S. Chen, S. Camp, K. J. Schafer, and M. B. Gaarde, Theory of strong-field attosecond transient absorption, J. Phys. B **49**, 062003 (2016).
[27] A. Stenquist, F. Zapata, and J. M. Dahlström, Gauge-invariant absorption of light from a coherent superposition of states, Phys. Rev. A **107**, 053106 (2023).
[28] J. C. Baggesen, E. Lindroth, and L. B. Madsen, Theory of attosecond absorption spectroscopy in krypton, Phys. Rev. A **85**, 013415 (2012).
[29] S. Pabst, A. Sytcheva, A. Moulet, A. Wirth, E. Goulielmakis, and R. Santra, Theory of attosecond transient-absorption spectroscopy of krypton for overlapping pump and probe pulses, Phys. Rev. A **86**, 063411 (2012).

[30] E. Allaria *et al.*, Highly coherent and stable pulses from the FERMI seeded free-electron laser in the extreme ultraviolet, Nat. Photonics **6**, 699 (2012).
[31] S. Nandi *et al.*, Observation of Rabi dynamics with a short-wavelength free-electron laser, Nature (London) **608**, 488 (2022).
[32] S. Nandi *et al.*, Generation of entanglement using a short-wavelength seeded free-electron laser, Sci. Adv. **10**, eado0668 (2024).
[33] See Supplemental Material at http://link.aps.org/supplemental/10.1103/PhysRevLett.133.063202 for details on the theoretical methods, which includes Refs. [34–37].
[34] C. Cohen-Tannoudji, J. Dupont-Roc, and G. Grynberg, *Atom—Photon Interactions: Basic Process and Appilcations*, 1st ed. (Wiley, New York, 1998), 10.1002/9783527617197.
[35] E. Olofsson and J. M. Dahlström, Photoelectron signature of dressed-atom stabilization in an intense XUV field, Phys. Rev. Res. **5**, 043017 (2023).
[36] V. Paulisch, H. Rui, H. K. Ng, and B.-G. Englert, Beyond adiabatic elimination: A hierarchy of approximations for multi-photon processes, Eur. Phys. J. Plus **129**, 12 (2014).
[37] F. H. M. Faisal, *Theory of Multiphoton Processes* (Springer US, Boston, MA, 1987).
[38] K.-H. Yang, Gauge transformations and quantum mechanics I. Gauge invariant interpretation of quantum mechanics, Ann. Phys. (N.Y.) **101**, 62 (1976).
[39] L. Allen and J. H. Eberly, *Optical Resonance and Two-Level Atoms* (Dover, New York, 1987).
[40] B. R. Mollow, Stimulated emission and absorption near resonance for driven systems, Phys. Rev. A **5**, 2217 (1972).
[41] A. Palacios, H. Bachau, and F. Martín, Step-ladder Rabi oscillations in molecules exposed to intense ultrashort VUV pulses, Phys. Rev. A **74**, 031402(R) (2006).
[42] S. Pan, C. Hu, W. Zhang, Z. Zhang, L. Zhou, C. Lu, P. Lu, H. Ni, J. Wu, and F. He, Rabi oscillations in a stretching molecule, Light Sci. Appl. **12**, 35 (2023).
[43] Y. Chen, S. Peng, Z. Fu, L. Qiu, G. Fan, Y. Liu, S. Wu, X. Xie, and Z. Tao, Ultrafast quantum control of atomic excited states via interferometric two-photon Rabi oscillations, Commun. Phys. **7**, 98 (2024).
[44] O. Postavaru, Fully relativistic description of the power spectrum, J. Opt. Soc. Am. B **35**, 2000 (2018).
[45] P. Stammer, J. Rivera-Dean, A. S. Maxwell, T. Lamprou, J. Argüello-Luengo, P. Tzallas, M. F. Ciappina, and M. Lewenstein, Entanglement and squeezing of the optical field modes in high harmonic generation, Phys. Rev. Lett. **132**, 143603 (2024).
[46] P. Stammer, J. Rivera-Dean, A. Maxwell, T. Lamprou, A. Ordóñez, M. F. Ciappina, P. Tzallas, and M. Lewenstein, Quantum electrodynamics of intense laser-matter interactions: A tool for quantum state engineering, PRX Quantum **4**, 010201 (2023).